Structural studies of the acetylcholine receptor in the membrane environment

Francisco J. Barrantes

UNESCO Chair of Biophysics and Molecular Neurobiology, Instituto de Investigaciones Bioquímicas de Bahía Blanca, 8000 Bahía Blanca, B8000FWB, Argentina

The nicotinic acetylcholine receptor (AChR) is the archetype molecule in the superfamily of ligand-gated ion channels. All members of this superfamily mediate fast intercellular communication in response to endogenous neurotransmitters. Here I review a series of biophysical studies on the AChR protein with particular focus on the interactions of the macromolecules with its lipid membrane microenvironment.

Spectroscopic studies of the micro-to-millisecond translational and rotational mobility of the AChR in the native membrane and synthetic lipid systems provide information on the dynamics of this protein in a two-dimensional lattice, the lipid bilayer. Motional regimes in the nanosecond time-scale can be explored with other techniques, such as electron spin resonance. Application of the latter technique led to the discovery of a lipid fraction in direct contact with the AChR, with rotational dynamics 50-fold slower than those of the bulk lipids. The lipid belt-region around the AChR molecule has since become the focus of a variety of investigations aimed at defining its possible role in the modulation of AChR function.

The polarity and molecular dynamics of solvent dipoles – mainly water – in the vicinity of the lipids in the AChR membrane have been studied with Laurdan extrinsic fluorescence, and Förster-type resonance energy transfer (FRET) was introduced to characterize the receptor-associated lipid microenvironment. FRET has been used to discriminate between the bulk lipid and the lipid belt-region in the vicinity of the protein. The AChR-vicinal lipid is in a liquid-ordered phase and exhibits a higher degree of order than the bulk bilayer lipid. Changes in FRET efficiency induced by fatty acids, phospholipid and cholesterol also led to the identification of discrete sites for these lipids on the AChR protein.

The topography of the AChR membrane-embedded domains has recently been explored with fluorescence methods using whole *Torpedo* AChR protein and transmembrane peptides. The location of pyrene maleimide-labeled Cys residues in transmembrane domains αM1, αM4, γM1 and γM4 was determined by differential fluorescence quenching with spin-labeled derivatives of various lipids. Pyrene-labeled Cys residues were found to lie in a shallow position. For M4 segments, this is in agreement with a predicted linear α-helix; for M1, it is necessary to postulate a substantial amount of non-helical structure, and/or of kinks, to rationalize the superficial location of Cys residues. Three evolutionarily conserved proline residues in M1 may account for such structure. Proline residues appear to be conserved in transmembrane segments of M1 in the AChR and all members of the rapid ligand-gated ion channel superfamily.

THE nicotinic acetylcholine receptor (AChR) is one of the best-characterized members of the ligand-gated ion channel (LGIC) superfamily[1], a set of proteins coded by more than a hundred genes identified so far. They exhibit amino acid sequence homology and presumably higher-order structural motifs. Within the LGIC superfamily, the AChR and a subtype of the serotonin (5-HT_3) receptor comprise two families of cation-selective channels, whilst glycine and $GABA_A$ receptors are anion-selective channels. Signal transduction is relatively fast and results from similar mechanistic steps: binding of the neurotransmitter followed by conformational transitions in the receptor proteins that lead to changes in the ionic permeability of the postsynaptic membrane. In the specific case of the AChR, upon binding, acetylcholine (ACh) initiates a conformational change in this protein that triggers the transient opening of its intrinsic cation-specific channel across the postsynaptic membrane. At the molecular level, this is accomplished by the concerted action of an array of four different but highly homologous AChR subunits in the stoichiometry $\alpha 2\beta\gamma\delta$ (refs 2–4).

Each AChR subunit contains four putative hydrophobic segments, 20–30 amino acids in length, referred to as M1–M4 and proposed to be membrane-spanning segments. The M2 segment from each subunit is thought to contribute structurally to form the ion channel proper. The M4 segment was proposed as the most likely candidate to be exposed to the bilayer lipid[5,6]. M1 and M3 effectively incorporate membrane-partitioning photoactivatable probes[7–9] and are likely to be exposed to the lipid phase as well. It is usually accepted that the four

e-mail: rtfjb1@criba.edu.ar

hydrophobic segments M1–M4 correspond to regions of the protein fully embedded in the membrane, and are referred to as transmembrane (TM) domains[9,10]. As to their secondary structure, the original postulation of an all (four)-helix bundle[11] has been challenged by the results of cryoelectron microscopy of frozen AChR tubules[12] and computer-aided molecular modeling indicating that the dimensions of the AChR TM region are not compatible with a pentameric four-helix bundle[13].

Only a very limited number of high-resolution structures of membrane proteins have been obtained to date using classical X-ray crystallography methods, mainly because of the difficulty of obtaining large well-ordered three-dimensional crystals. Two-dimensional arrays adequate for electron diffraction techniques are available for a few membrane proteins. The crystal structure of a water-soluble ACh-binding protein from a snail has appeared very recently[14].

This soluble AChR-like protein is released into the synaptic region in a molluscan cholinergic synapse in response to the natural agonist ACh. The protein traps ACh and thus suppresses synaptic transmission. The release of this decoy glial receptor protein into the synaptic cleft provides a novel mechanism by which glial cells can modulate the efficacy of cholinergic neurotransmission. The structure of this protein, highly homologous to the water-soluble extracellular domain of the AChR protein proper[14], provides the first putative high-resolution views of the region of the AChR involved in agonist recognition, the first step in the cascade leading to channel opening in the cholinergic synapse. This exciting development is bound to lead to new insights into the mechanisms of fast signal transduction in general.

Site-directed mutagenesis data combined with patch-clamp electrophysiology, and results from photoaffinity labelling with noncompetitive channel blockers, support the notion that the M2 domain lines the walls of the pore and are indicative of α-helical periodicity in the residues exposed to the lumen of the AChR channel[15]. NMR studies of the M2 segment of the δ subunit[16] indicate that this domain is inserted in the bilayer at an angle of 12° relative to the membrane normal, in totally α-helical configuration. A synthetic peptide corresponding to the *Torpedo* αM2 segment in chloroform: methanol containing $LiClO_4$ also adopts a totally α-helical configuration[17].

Cryoelectron microscopy has so far revealed a relatively featureless appearance of the other putative TM domains (M1, M3 and M4). A large portion of this AChR region is postulated to be arranged in the form of a β-barrel outside the central rim of M2 channel-forming rods[12]. This interpretation is in contrast with photoaffinity labelling studies, in which the observed periodicity of the lipid-exposed residues in M4 and M3 is consistent with an α-helical pattern[8,9,18] and with deuterium-exchange Fourier transform infrared spectroscopy studies which indicate a predominantly α-helical structure in the AChR TM region[19]. In addition, secondary structure analysis (CD and Fourier transform infrared spectroscopy) of isolated and lipid-reconstituted TM AChR peptides indicates α-helical structure for M2, M3, and M4 segments[20]. Furthermore, a synthetic peptide corresponding to the αM3 segment of *Torpedo* AChR exhibited a totally α-helical structure by 2-dimensional ^{1}H-NMR spectroscopy[21], and a recent NMR study of a synthetic γM4 peptide is also compatible with an α-helical secondary structure[22].

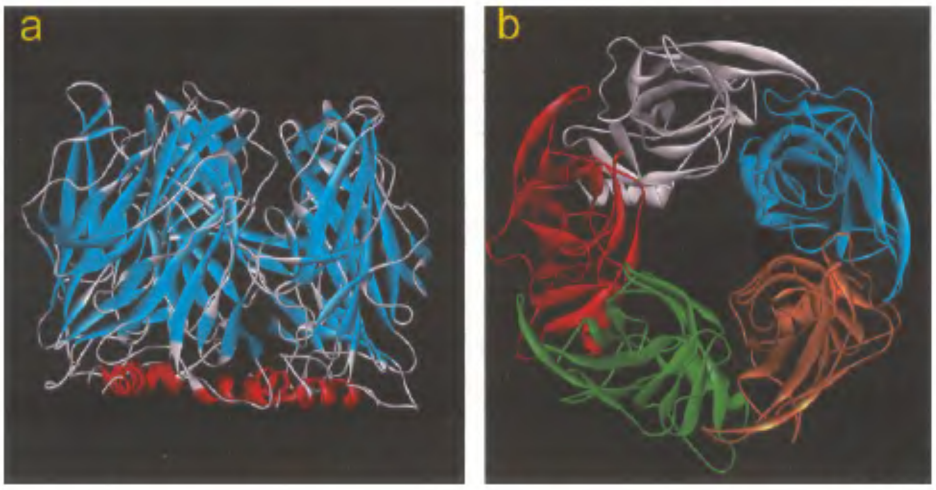

Figure 1. Crystal structure of an ACh-binding protein[14] highly homologous to the extracellular region of the AChR. The ACh-binding protein was found in a molluscan cholinergic synapse. This water-soluble protein is released into the synaptic region in response to the natural agonist ACh. It thus functions as a molecular decoy, capturing ACh and thus suppressing synaptic transmission. Atomic coordinates are deposited at the Brookhaven Protein Data Bank with accession number 1I9B.

Another area of research in which protein–AChR interactions might be involved is that of the stabilization of receptor aggregates, or 'clusters'. Prior to innervation, the AChR is uniformly distributed on the cell surface. In the course of synaptogenesis, the AChR becomes clustered first in the form of 'hot spots' and finally, upon establishment of the neuromuscular junction, receptor molecules adopt the high-density packing characteristic of the adult synapse. It is not known whether the different organizational modes of the AChR protein are accompanied by large-scale modifications of their lipid environment. We do know, however, that the closely associated lipid belt region surrounding the AChR protein in the electrolyte is qualitatively different in terms of molecular mobility[23], and the lipid composition of the synaptic region has been reported to differ from that of the rest of the membrane in muscle cells[24].

This review evaluates the impact of some biophysical studies of the lipid–AChR interactions on our current knowledge of structural and dynamic properties of the AChR molecule in its membrane environment.

AChR–lipid interactions

Early electron spin resonance (ESR) studies by Marsh and Barrantes[23] and Marsh *et al.*[25] determined the occurrence of direct interactions between lipid and AChR in its native membrane environment. This series of studies demonstrated that the protein-associated or 'annular' lipids were relatively immobile with respect to the rest of the membrane lipids, a finding confirmed by other laboratories[26,27] using AChR reconstituted into lipid systems.

The need to include sterols and certain phospholipids to preserve AChR functionality in reconstituted systems was subsequently demonstrated[28]. The different contributions of phospholipid and sterol could be established in various studies *in vitro*[29–31] and the minimal number of lipid molecules (~ 45) per AChR was ascertained in ESR experiments[27,32]. AChR-vicinal (annular) lipids were thus shown to be important for the correct functioning of the AChR, but the details of the interaction were still obscure.

Dynamics of AChR and lipids in the membrane

2D-translational dynamics of the AChR in cells and synthetic membranes

The Stokes–Einstein treatment of motion of a body in a solvent medium considers lateral motion as originating in random collisions of the body with the solvent molecules, a phenomenon that is opposed by frictional forces between the two. When relatively large integral membrane proteins like the AChR, whose dimensions generously exceed those of the surrounding lipids, are reconstituted into artificial bilayers at relatively low protein: lipid ratios, the lateral diffusion of the protein can be approximated by the Saffman and Delbruck[33] formalism. The free diffusion coefficient of a particle in a free-volume model, D_t, is given by $D + kT/f$, where k is the Boltzmann constant and f is the frictional coefficient. In the case of a spherical molecule of hydrodynamic radius r diffusing in a medium of viscosity η, $D = kT/6\pi\eta r$ (the Stokes–Einstein equation). Saffman and Delbruck applied this formalism to the case of a cylinder of radius r oriented perpendicular to and diffusing in a thin viscous sheet of viscosity η and thickness h (equal to the height of the embedded cylinder), a treatment that is more relevant to that of a protein transversing a membrane. The diffusion coefficient in the Safman–Delbruck formalism becomes:

$$D = (kT/4\pi\eta_m h)\ln(\eta_m h/\eta_w r - 0.577), \quad (1)$$

where η_m is the viscosity of the viscous sheet (the membrane) and η_w ($\approx 10 \times^{-2}$ poise) is the viscosity of the aqueous medium in which the sheet is immersed. The two media that bathe the molecule, i.e. the membrane and water, will produce different shear forces on the membrane-embedded and water-exposed regions of the macromolecules, respectively. The transmembrane mass of the protein, embedded in a lipid of much higher viscosity than water, is more important in determining the lateral mobility of the protein; large deletions of membrane-embedded integral proteins have little effect on their translational dynamics. The membrane is treated as a continuum of solvent molecules. The formalism predicts a weak dependence of D on protein radius, a prediction that appears to be followed roughly by the integral membrane proteins studied to date, including the AChR[30]. It should be noted that the theory finds validity only in the case of very diluted proteins (such as with proteins reconstituted in lipid bilayers).

Variations of the fluorescence recovery after photobleaching (FRAP) technique have been developed and applied to various membrane proteins, including the AChR. These experiments provide useful information on the dynamics of the mobile fraction of the AChR particles in the membrane and also report on the fraction of immobile receptors. In fact the latter appears to be a substantial portion of the total in adult and embryonic muscle cells. FRAP studies have revealed that the AChR in the adult synapse and in the patches in developing muscle is translationally immobile, whereas the non-synaptic areas have AChRs with a higher diffusion coefficient, of about 5×10^{-11} cm^2 s^{-1} (refs 34–38).

We studied the lateral diffusion of detergent-solubilized AChR reconstituted in pure dimyristoylphosphatidylcholine bilayers, and found values of D_t in the range of 10^{-8} cm^2 s^{-1} for both the AChR monomer

and dimer in the liquid-crystalline phase and within the 14–37°C range[30]. Additional multiple component recoveries with D_t of less than 5×10^{-11} cm^2 s^{-1} were found below the lipid phase transition. Thus in the low concentration limit, neither the 9S AChR monomer nor the 13S dimer of about half-a million Daltons molecular weight devoid of rapsyn and other peripheral non-receptor proteins encounter hindrance to lateral diffusion on the part of the lipid bilayer itself, whereas in native membranes, the densely packed AChR molecules are almost totally anchored and both translational and rotational diffusion are inhibited. To put these figures in perspective, the fluorescent lipid analog NBD-phosphatidylethanolamine, for instance, exhibits values of D_t, the lateral diffusion coefficient, of 8×10^{-8} cm^2 s^{-1} (ref. 30)

In the plasmalemma of developing rat myotubes, two populations of AChR molecules are observed: a diffusely distributed population having $D_t = 5 \times 10^{-11}$ cm^2 s^{-1} and a localized, patched population with $D_t \approx 10^{-12}$ cm^2 s^{-1} (ref. 34). When blebs are produced in myoblast sarcolemma, D_t is even faster (3×10^{-9} cm^2 s^{-1}, ref. 35). Lack of hindrance to diffusion was also reported for AChR in the plasma membrane of *Xenopus* embryonic myoblasts, where Poo[36] estimated D_t to be = 2.6×10^{-9} cm^2 s^{-1}. D_t in reconstituted membranes is at least 50-fold higher than the highest values found in native membranes. This means that the AChR undergoes essentially free lateral diffusion, i.e. Brownian motion, in a synthetic lipid bilayer, whereas in native membranes or in living cells it exhibits various degrees of hindrance of motion. Reconstituted membranes differ from natural membranes in their lipid composition, concentration of protein, and absence of peripheral and cytoskeletal proteins. The former factor was not found to influence the lateral diffusion of the AChR at very high lipid: protein ratios. It is likely that the extensive protein–protein interactions occurring both between AChR molecules on the one hand and between AChR molecules and cytoskeletal and other non-receptor proteins like rapsyn on the other, are mainly responsible for the relative immobilization of AChR in native membranes and particularly in the synaptic region.

Rotational dynamics of the AChR

Rotational motion of the AChR protein has been studied by means of ESR and phosphorescence anisotropy techniques. A spectrum of relaxation times is observed with both methods; the rotational correlation time ϕ of the monomeric AChR is about 10–25 μs (ref. 39), in full agreement with the expected value. Slower relaxation times are probably related to the existence of higher oligomeric AChR species. Early ESR studies[23,25,27,40] showed the rotational immobility of the AChR protein in native AChR-rich membranes purified from fish electric organ. Other studies[41,42] focused on the rotational motion of the AChR in membranes by studying the phosphorescence anisotropy of AChR labelled with an erythrosine derivative of α-bungarotoxin. We employed eosin derivatives of the α-toxin, and observed a finite rotational correlation time of 12–26 μs for the AChR in native membranes[39], in agreement with that expected for the 9S AChR monomer of about 250,000 Da. For an ideal spherical particle with a volume proportional to its molecular mass, M, one can further predict that the translational diffusion coefficient is proportional to the inverse of the cube root of the molecular mass: $D_t \sim M^{-1/3}$. Since the translational motion of the AChR in reconstituted pure lipid bilayers can for practical reasons be considered a free, unrestricted Brownian motion-type lateral diffusion (see above), D_t can also be related to the rotational relaxation time by $D_t \approx 4r^2/\phi$.

Physical state of the AChR–lipid interface

The AChR is in a liquid-ordered phase in the native membrane

The so-called Generalized Polarization (GP) (see refs 47, 48) of the fluorescent probe Laurdan (6-dodecanoyl-2-dimethylamino naphthalene, Figure 3) has been used to learn about the dynamics of the AChR and some physical properties of the protein-vicinal lipid[43,44]. Towards this end we introduced a hitherto unexploited property of Laurdan, namely its ability to act as a Förster-type resonance energy transfer (FRET) acceptor of tryptophan emission.

Laurdan is a particularly advantageous fluorescent probe; its spectral properties are extremely sensitive to the polarity and to the molecular dynamics of dipoles in its environment. This is due to dipolar relaxation processes that are reflected as relatively large spectral shifts. Laurdan GP reports on the polarity and dynamics of the solvent dipoles in its surroundings. The main dipoles sensed by Laurdan in the membrane are water molecules. When no relaxation occurs, high GP values result, indicative of low water content in the hydrophilic/hydrophobic interface region of the membrane. In particular, the temperature dependence of Laurdan GP has been utilized to describe and to quantify the phase states of membrane systems. Moreover, by studying the behavior of Laurdan fluorescence under different excitation/emission wavelengths it has been possible to characterize qualitatively the phase state of native and artificial membrane systems[46].

Studies of Laurdan GP showed that the AChR–lipid interface region, i.e. the AChR–vicinal lipid, exhibits a higher rigidity compared to that in the rest of the

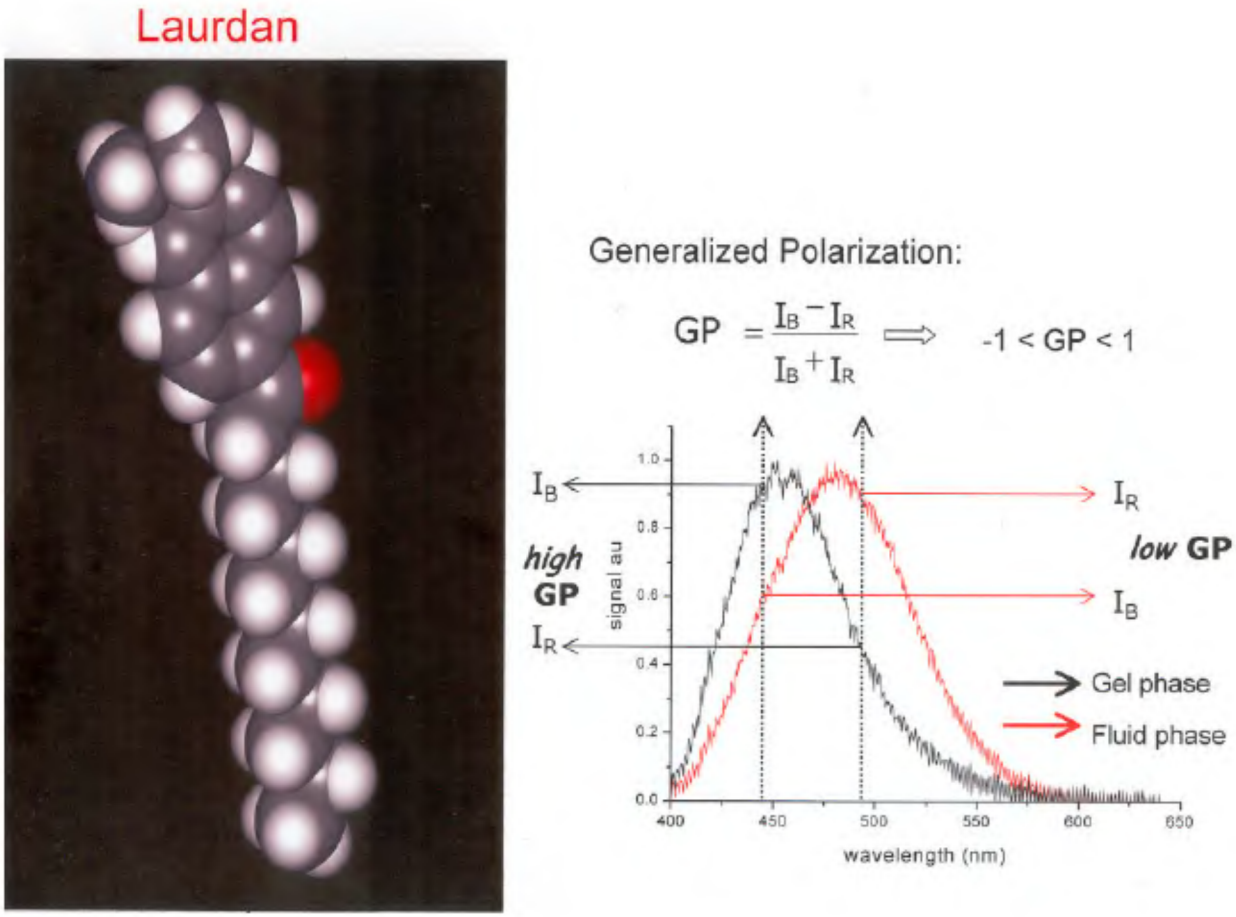

Figure 2. Molecular model of the environmentally sensitive fluorescent probe Laurdan (6-dodecanoyl-2-dimethylamino naphthalene). Of particular interest in our studies is the use of the so-called General Polarization (GP) of Laurdan[45,46], given by $GP = (I_B - I_R)/(I_B + I_R)$, where I_B (434 nm) and I_R (490 nm) are the Laurdan fluorescence intensities at the blue and red edges of the emission spectrum, respectively. We have introduced the use of Laurdan in FRET experiments, exploiting its ability to form an ideal acceptor of intrinsic protein fluorescence[43,44]. GP values observed under energy transfer conditions exhibit higher absolute values than those obtained by direct excitation of the probe, indicating the lower polarity of the lipid in the microenvironment of the AChR protein.

membrane bilayer, although a single thermotropic phase with the characteristic of the so-called liquid-ordered phase defines the AChR-rich postsynaptic membrane of fish electrocytes[43].

Laurdan GP correlates with energetics of channel gating in living cells

The characterization of Laurdan thermotropic behaviour was subsequently extended to living mammalian cells expressing endogenous or heterologous AChR. Interestingly, the differences in physical properties of cell membranes measured by Laurdan GP in a variety of cells, reflecting the molecular dynamics of water molecules, could be correlated with the energetic changes in the AChR ion channel occurring as a function of temperature, as measured in single-channel recordings[47]. Laurdan expends energy in solvent (water) reorientation, as evidenced in the red shift of its emission spectrum. The decrease in Laurdan GP upon increasing the temperature reflects the increase in water diffusion into the membrane. Water diffusion is facilitated by the increased thermal-induced disorder in the bilayer lipid. The higher AChR channel conductance upon increasing the temperature is a manifestation of the augmented ion and water permeability in the AChR channel or 'pore' region as we observed in single-channel recordings with the patch-clamp technique. Our study[47] indicates that AChR channel kinetics depends not only on intrinsic properties of the AChR protein but also on the physical state of the membrane in which the receptor is embedded.

Lipids modulate the fluidity of the AChR microenvironment

Studies from the group of McNamee[48,49] show that reconstituted AChR is sensitive to the bulk fluidity of the membrane, as measured by ion flux experiments. When Laurdan GP was measured in *Torpedo* native AChR

membrane by direct excitation or under FRET conditions in the presence of exogenous lipids, GP, and by inference the 'fluidity' and order of the membrane, were found to diminish upon addition of oleic acid and DOPC, and not to vary significantly upon addition of cholesterol hemisuccinate, indicating an increase in the polarity of the single, ordered-liquid lipid phase in the two former cases[44].

Complementary information about the bulk lipid order was obtained from measurements of fluorescence anisotropy of DPH and two of its derivatives. The membrane order diminished in the presence of oleic acid and DOPC. The location of Laurdan was determined using the parallax method of Chattopadhyay and London[50]. Their method is based on the relative position of a fluorescence probe embedded in the membrane and its quenching by probes having nitroxide spin labels at different positions along their acyl chains. The parallax determination is accomplished by pairwise comparison of quenching parameters with different pairwise combinations of the PC analogs with spin labels in carbons 7, 10 and 12. Using this approach, Laurdan was found to lie at ~ 10 Å from the center of the bilayer, i.e. at depth of ~ 5 Å from the lipid–water interface[44]. In previous work from our laboratory a minimum donor–acceptor distance of 14 ± 1 Å was calculated for the Laurdan-AChR pair in the *Torpedo* native membrane[43], in agreement with the overall dimensions of the AChR and its transmembrane region in particular (see ref. 1).

Lipid sites at the lipid–AChR interface

Fatty acids[51–53], phospholipids containing short-chain fatty acids[54], and steroids[55–57] have been shown to exert effects on AChR function. Fatty acids and dioleylphosphatidylcholine decrease GP of bulk and lipid belt-regions in the native AChR membrane, whereas a cholesterol ester does not. This is in agreement with fluorescence quenching studies with brominated lipids that identified annular sites for phospholipids and non-annular sites for cholesterol, both accessible to fatty acids[58,59].

We subsequently introduced a new strategy for determining lipid–AChR interactions in AChR-rich membranes[44]. The approach consists in measuring the decrease in the energy transfer efficiency (E) between the intrinsic fluorescence of AChR-rich membranes and Laurdan, induced by different lipids. E between AChR (donor) and Laurdan (acceptor) was calculated using eqs 2 and 3. According to Förster's theory[60], E is given by:

$$E = R_0^6/(R_0^6 + r^6), \quad (2)$$

where r is the intermolecular distance and R_0 is a constant parameter for each donor–acceptor pair, defined as the distance at which E is 50%. E can also be calculated as:

$$E = 1 - (\phi/\phi_D) \approx 1 - (I/I_D), \quad (3)$$

where ϕ and ϕ_D are the fluorescence quantum yields of donor in the presence and absence of the acceptor, respectively, and I and I_D are the corresponding emission intensities. FRET efficiency was found to decrease upon addition of exogenous lipids, which displace Laurdan molecules from the AChR-microenvironment. The maximal decrease in E resulting from the addition of a fatty acid (18 : 1) amounted to about 60%, whereas cholesterol or phospholipid reduced E by 35% and 25%, respectively. The sum of the decrease caused by DOPC and CHS equaled that obtained in the presence of 18 : 1 alone. From this series of experiments we reached the conclusion that there are independent sites for phospholipid and sterol, both accessible to fatty acid, in the vicinity of the AChR[44].

Topography of AChR membrane-embedded domains

We have recently prepared transmembrane (TM) peptides from purified *Torpedo californica* AChR protein by controlled enzymatic digestion, and derivatized with N-(1-pyrenyl-maleimide (PM), purified, and reconstituted these peptides into asolectin liposomes[61]. PM labelling occurred in cysteine residues in αM1, αM4, γM1 and γM4. The labelled cysteine residues are in all cases exposed to the surrounding lipid and located at the 'cytoplasmic' end of the AChR TM region, in fact very close to the bilayer–water interface (Figure 3).

The topography of the pyrene-labeled Cys residues with respect to the membrane was experimentally determined by differential fluorescence quenching with spin-labelled derivatives of fatty acids, phosphatidylcholine, and the steroids cholestane and androstane. Stern-Volmer plots of whole AChR quenching by spin-labelled lipid analogs showed no deviation from linearity. Stearic acid and androstane spin label derivatives were the most effective quenchers of the pyrene fluorescence of whole AChR and derived TM peptides. In the case of spin-labelled stearic acid derivatives, the 5-SASL isomer quenched more effectively than the 7-SASL and the 12-SASL analogs, indicating a shallow location of the pyrene-labelled Cys residues.

In fact, the quenching studies were compatible with the occurrence of shallow positions for all labelled Cys residues in the AChR and derived TM peptides. In the case of γM4, and by interface in other M4 segments of the AChR, this is compatible with a linear α-helical structure (Figure 4). In the case of αM1, 'classical' models locate Cys^{230} at the center of the bilayer in an

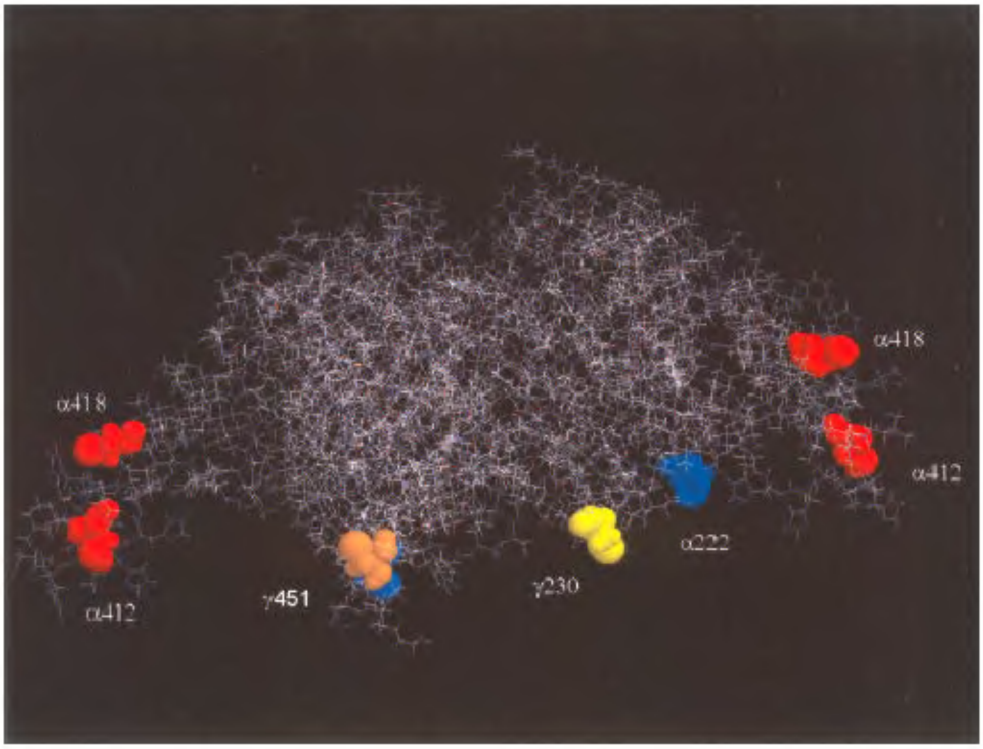

Figure 3. Molecular model of the AChR transmembrane domain outlining the location of the pyrene-labelled cysteine residues. The model was drawn using the atomic coordinates of ref. 62 and the software WebLab Viewer from Molecular Simulations, Inc. All cysteine residues in the TM AChR domain are closer to the cytoplasmic-facing region of the membrane (bottom part of the picture) and occupy superficial positions in the transmembrane domain, thus being readily exposed to the surrounding lipid.

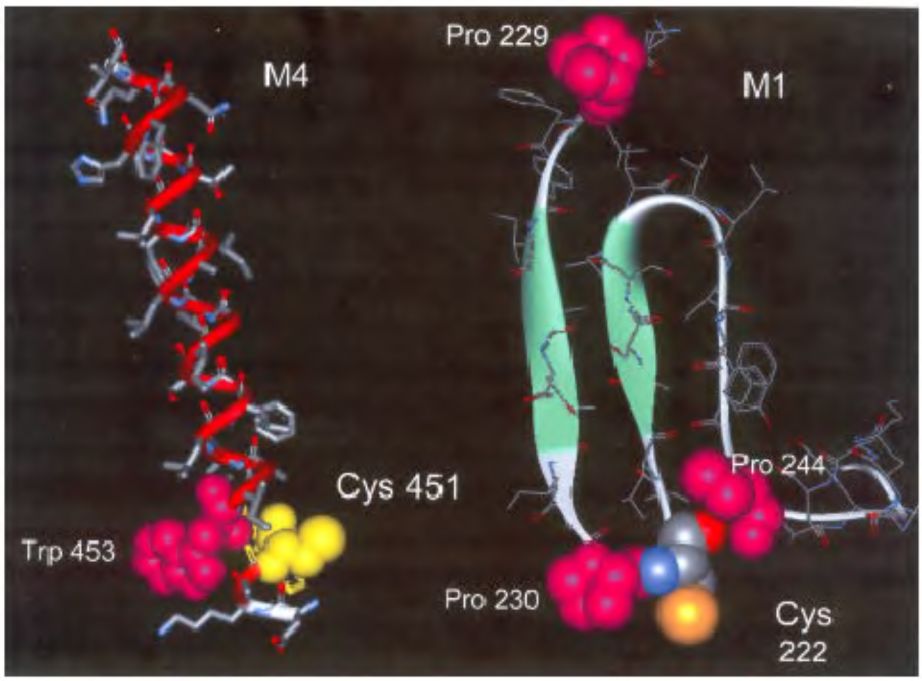

Figure 4. Molecular model of representative structures of M4-type and M1-type AChR transmembrane regions compatible with recent fluorescence experimental data[61]. Cys^{451} is located very close to the cytoplasmic-facing end of αM4, and relatively close to Trp^{453}. Notice the presence of three proline residues along M1 (Pro^{230} and Pro^{244} close to the cytoplasmic end and to Cys^{222}, and Pro^{229}, close to the extracellular-facing end of M1). Helix-breaking proline residues appear to be evolutionarily conserved in M1 regions of the AChR and other members of the LGIC. Drawn using the software WebLab Viewer from Molecular Simulations, Inc. using the coordinates of ref. 62.

extended α-helical structure. This is not compatible with the shallow location of pyrene-labelled Cys^{230} emerging from the experimental results. The transmembrane topography of M1 can be explained on the basis of the presence of a substantial amount of non-helical structure, and/or of kinks along M1 (Figure 4).

In a mixed α-helix/β-sheet model of the AChR (ref. 62), αM1 was constructed as a three-strand β-sheet interrupted by short loops generated by searching in the database of known structures for an appropriate backbone conformation. The proline residues themselves cannot be found within a β-strand, so they were positioned in the loops. The same model can be extended to γM1, having a proline residue (Pro^{229}) immediately adjacent to Cys^{230} and two other (Pro^{222} and Pro^{244}) at the end of the TM region. Thus, the conserved proline residues in the M1 segments of the AChR might introduce 'curls' or kinks (Figure 4) in a manner analogous to that recently reported for one of the transmembrane segments of a K^+ channel[63]. In the case of the γM1 fragment there appears to be no detailed information on its topography in the membrane as yet, but the occurrence of helix-interrupting proline residues is a striking feature of M1 in the AChR and all members of the rapid ligand-gated ion channel superfamily.

1. Barrantes F. J. (ed.), *The Nicotinic Acetylcholine Receptor: Current Views and Future Trends*, Springer Verlag, Berlin, Georgetown, TX, 1998, p. 226.
2. Reynolds, A. and Karlin, A., *Biochemistry*, 1978, **17**, 2035–2038.
3. Lindstrom, J., Merlie, J. P. and Yogeeswaram, G., *Biochemistry*, 1979, **18**, 4465–4470.
4. Raftery, M. A., Hunkapiller, M. W., Strader, C. D. and Hood, L. E., *Science*, 1980, **208**, 1454–1457.
5. Giraudat, J., Montecucco, C., Bisson, R. and Changeux, J.-P., *Biochemistry*, 1985, **24**, 3121–3127.
6. Tobimatsu, T., Fujita, Y., Fukuda, K., Tanaka, K., Mori, Y., Konno, T., Mishina, M. and Numa, S., *FEBS Lett.*, 1987, **222**, 56–62.
7. Blanton, M. P. and Wang, H. H., *Biochim. Biophys. Acta*, 1991, **1067**, 1–8.
8. Blanton, M. P. and Cohen, J. B., *Biochemistry*, 1992, **31**, 3738–3750.
9. Blanton, M. P. and Cohen, J. B., *Biochemistry*, 1994, **33**, 2859–2872.
10. Chavez, R. A. and Hall, Z. W., *J. Cell Biol.*, 1992, **116**, 385–393.
11. Noda, M. Takahashi, H., Tanabe, T., Toyosato, M., Kikyotani, S., Hirose, T., Asai, M., Takashima, H., Inayama, S., Miyata, T. and Numa, S., *Nature*, 1983, **299**, 793–797.
12. Unwin, N., *Nature*, 1995, **373**, 37–43.
13. Ortells, M. O., Barrantes, G. E. and Barrantes, F. J. (ed.), *The Nicotinic Acetylcholine Receptor: Current Views and Future Trends*, Springer Verlag, Berlin, Georgetown, pp. 85–108.
14. Brejc, K., van Dijk, W. J., Klaassen, R. V., Schuurmans, M., van der Oost, J., Smit, A. B. and Sixma, T. K., *Nature*, 2001, **411**, 269–276.
15. Changeux, J. P. and Edelstein, S. J., *Neuron*, 1998, **21**, 959–980.
16. Opella, S. J., Marassi, F. M., Gesell, J. J., Valente, A. P., Kim, Y., Oblatt-Montal, M. and Montal, M., *Nature Struct. Biol.*, 1999, **6**, 374–379.
17. Pashkov, V. S., Maslenikov, I. V., Tchikin, L. D., Efremov, R. G., Ivanov, V. T. and Arseniev, A. S., *FEBS Lett.*, 1999, **457**, 117–121.
18. Blanton, M. P., McCardy, E. A., Huggins, A. and Parikh, D., *Biochemistry*, 1998, **37**, 14545–14555.
19. Baenziger, J. E. and Méthot, N., *J. Biol. Chem.*, 1996, **270**, 29129–29137.
20. Corbin, J., Méthot, N., Wang, H. H., Baenziger, J. E. and Blanton, M. P., *J. Biol. Chem.*, 1998, **273**, 771–777.
21. Lugovskoy, A. A., Maslennikov, I. V., Utkin, Y. N., Tsetlin, V. I., Cohen, J. B. and Arseniev, A. S., *Eur. J. Biochem.*, 1998, **255**, 455–461.
22. Williamson, P. F., Bonev, B., Barrantes, F. J. and Watts, A., *Biophys. J.*, 2000, **78**, A147.
23. Marsh, D. and Barrantes, F. J., *Proc. Natl. Acad. Sci. USA*, 1978, **75**, 4329–4333.
24. Bloch, R. J. and Morrow, J. S., *J. Cell Biol.*, 1989, **108**, 481–494.
25. Marsh, D., Watts, A. and Barrantes, F. J., *Biochim. Biophys. Acta*, 1981, **645**, 97–101.
26. Rousselet, A., Devaux, P. F. and Wirtz, K. W., *Biochem. Biophys. Res. Commun.*, 1979, **90**, 871–877.
27. Ellena, J. F., Blazing, M. A. and McNamee, M. G., *Biochemistry*, 1983, **22**, 5523–5535.
28. Epstein, M. and Racker, E., *J. Biol. Chem.*, 1978, **253**, 6660–6662.
29. Ochoa, E. L., Dalziel, A. W. and McNamee, M. G., *Biochim. Biophys. Acta*, 1983, **727**, 151–162.
30. Criado, M., Eibl, H. and Barrantes, F. J., *Biochemistry*, 1982, **21**, 3622–3629.
31. Criado, M., Eibl, H. and Barrantes, F. J., *J. Biol. Chem.*, 1984, **259**, 9188–9198.
32. Jones, O. T., Eubanks, J. H., Earnest, J. P. and McNamee, M. G., *Biochemistry*, 1988, **27**, 3733–3742.
33. Saffman, P. G. and Delbrück, M., *Proc. Natl. Acad. Sci. USA*, 1975, **72**, 2035–2038.
34. Axelrod, D., Koppel, D. E., Schlessinger, J., Elson, E. and Webb, W. W., *Biophys. J.*, 1976, **16**, 1055–1069.
35. Tank, D. W., Wu, E.-S. and Webb, W. W., *J. Cell Biol.*, 1982, **92**, 207–212.
36. Poo, M.-M., *Nature*, 1982, **295**, 332–334.
37. Axelrod, D., Ravdin, P. M. and Podleski, T. R., *Biochim. Biophys. Acta*, 1978, **511**, 23–38.
38. Axelrod, D., Wright, A., Webb, W. W. and Horitz, A., *Biochemistry*, 1979, **17**, 3604–3609.
39. Bartholdi, M., Barrantes, F. J. and Jovin, T. M., *Eur. J. Biochem.*, 1981, **120**, 387–389.
40. Rousselet, A. and Devaux, P. F., *Biochem. Biophys. Res. Commun.*, 1977, **78**, 448–454.
41. Lo, M. M. S., Garland, P. B., Lamprecht, J. and Barnard, E. A., *FEBS Lett.*, 1980, **111**, 407–412.
42. Rousselet, A., Cartaud, J. and Devaux, P. F., *Biochim. Biophys. Acta*, 1981, **648**, 169–185.
43. Antollini, S. S., Soto, M. A., Bonini de Romanelli, I., Gutierrez-Merino, C., Sotomayor, P. and Barrantes, F. J., *Biophys. J.*, 1996, **70**, 1275–1284.
44. Antollini, S. S. and Barrantes, F. J., *Biochemistry*, 1998, **37**, 16653–16662.
45. Parasassi, T., De Stasio, G., d'Ubaldo, A. and Gratton, E., *Biophys. J.*, 1990, **57**, 1179–1186.
46. Parasassi, T., De Stasio, G., Ravagnan, G., Rusch, R. M. and Gratton, E., *Biophys. J.*, 1991, **60**, 179–189.
47. Zanello, L. P., Aztiria, E., Antollini, S. S. and Barrantes, F. J., *Biophys. J.*, 1996, **70**, 2155–2164.

48. Fong, T. M. and McNamee, M. G., *Biochemistry*, 1987, **26**, 3871–3880.
49. Sunshine, C. and McNamee, M. G., *Biochim. Biophys. Acta*, 1994, **1191**, 59–64.
50. Chattopadhyay, A. and London, E., *Biochemistry*, 1987, **26**, 39–45.
51. Andreasen, T. J., Doerge, D. R. and McNamee, M. G., *Arch. Biochem. Biophys.*, 1979, **194**, 468–480.
52. Andreasen, T. J. and McNamee, M. G., *Biochemistry*, 1980, **19**, 4719–4726.
53. Bouzat, C. B. and Barrantes, F. J., *Receptors Channels*, 1993, **1**, 251–258.
54. Braun, M. S. and Haydon, D. A., *Pflugers Arch.*, 1991, **418**, 62–67.
55. Bouzat, C. B. and Barrantes, F. J., *NeuroRep.*, 1993, **4**, 143–146.
56. Bouzat, C. B. and Barrantes, F. J., *Mol. Neuropharm.*, 1993, **3**, 109–116.
57. Bouzat, C. B. and Barrantes, F. J., *J. Biol. Chem.*, 1996, **271**, 25835–25841.
58. Jones, O. T. and McNamee, M. G., *Biochemistry*, 1988, **27**, 2364–2374.
59. Narayanaswami, V. and McNamee, M. G., *Biochemistry*, 1993, **32**, 12420–12427.
60. Förster, Th., *Ann. Phys. (Leipzig)*, 1948, **2**, 55–75.
61. Barrantes, F. J., Antollini, S. S., Blanton, M. P. and Prieto, M., *J. Biol. Chem.*, 2000, **275**, 37333–37339.
62. Ortells, M. O. and Lunt, G. G., *Prot. Eng.*, 1996, **9**, 51–59.
63. del Camino, D., Holmgren, M., Liu, Y. and Yellen, G., *Nature*, 2000, **403**, 321–325.

ACKNOWLEDGEMENTS. The experimental work quoted in this review was supported by grants from the Universidad Nacional del Sur, the Agencia Nacional de Promoción Científicay Tecnológica, Argentina, FIRCA 1-RO3-TW01225-01 and Antorchas/British Council to F.J.B.